Neuron, Vol. 37, 67–73, January 9, 2003, Copyright ©2003 by Cell Press

In Vivo Time-Lapse Imaging of Synaptic Takeover Associated with Naturally Occurring Synapse Elimination

Mark K. Walsh and Jeff W. Lichtman*
Department of Anatomy and Neurobiology
Washington University School of Medicine
Saint Louis, Missouri 63110

Summary

During development, competition between axons causes permanent removal of synaptic connections, but the dynamics have not been directly observed. Using transgenic mice that express two spectral variants of fluorescent proteins in motor axons, we imaged competing axons at developing neuromuscular junctions in vivo. Typically, one axon withdrew progressively from postsynaptic sites and the competing axon extended axonal processes to occupy those sites. In rare instances when the remaining axon did not reoccupy a site, the postsynaptic receptors rapidly disappeared. Interestingly, the progress and outcome of competition was unpredictable. Moreover, the relative areas occupied by the competitors shifted in favor of one axon and then the other. These results show synaptic competition is not always monotonic and that one axon's contraction in synaptic area is associated with another axon's expansion.

Introduction

During development, competition between axons causes the removal of some axonal connections and the maintenance of others (Katz and Shatz, 1996; Lohof et al., 1996; Purves and Lichtman, 1980). This phenomenon helps shape the pattern of neural circuits in many parts of the nervous system. We sought to directly image this competitive process to determine the time course and structural changes that accompany axon elimination and see if structural alterations in the remaining input might accompany the elimination of a competitor. This latter question was prompted by the observation that during development, axonal connections that are retained become progressively more powerful as other inputs are eliminated (Chen and Regehr, 2000; Colman et al., 1997; Jackson and Parks, 1982; Lichtman, 1977; Mariani and Changeux, 1981). We developed time-lapse techniques to study this form of synaptic plasticity in vivo using transgenic mice in which subsets of neurons express different fluorescent proteins (Feng et al., 2000). The use of multiple colors is critical because axons tend to be so closely juxtaposed with their competitors that they are not individually resolvable when labeled the same. In this way, terminal arbors of different axons converging on the same postsynaptic cell could be individually identified and monitored with time-lapse imaging over the developmental period when synapse elimination was taking place.

*Correspondence: jeff@pcg.wustl.edu

Results

Watching Synapse Elimination In Vivo

Transgenic mouse lines that expressed either Cyan Fluorescent Protein (CFP) or Yellow Fluorescent Protein (YFP) in all motor axons were mated to mice that expressed Green Fluorescent Protein (GFP) or CFP, respectively, in subsets of motor axons. In the resulting double transgenic progeny, all motor axons express one fluorescent protein, and a subset of motor axons additionally express a second spectrally distinct color (Figure 1A). At 1 week of age, we were able to find neuromuscular junctions in the sternomastoid muscles of these double transgenic mice that were innervated by two inputs that fluoresced different colors (Figure 1B). Several results suggest that these fluorescent axon terminals undergo synapse elimination normally. First, in the beginning of the second postnatal week, as in wild-type mice (Balice-Gordon and Lichtman, 1993), approximately half of the junctions were already singly innervated. Second, as in wild-type mice (Gan and Lichtman, 1998), those junctions that were still multiply innervated were contacted by two inputs and these appeared to be segregated into largely nonoverlapping regions of the junction (e.g., Figure 1B and see below). Third, as in wild-type mice (Balice-Gordon and Lichtman, 1993), there was almost a complete absence of multiply innervated junctions in the third postnatal week ($<$1%, 21 out of 3576 junctions).

Of approximately 1000 mouse pups screened, 25 had suitable (i.e., optically accessible) multiply innervated neuromuscular junctions. From these mice, 24 two-color (YFP and CFP or CFP and GFP) multiply innervated junctions and 4 multiply innervated one-color (YFP) junctions (segregated to the point that the two inputs could be unambiguously distinguished) were successfully monitored until they became singly innervated. The axons expressing both the subset fluorescent protein and the other color fluorescent protein that labeled all the axons were not more likely to remain or be eliminated than the axons that did not express the subset fluorescent protein. In 9/24 of the two-color junctions, the axon expressing the subset fluorescent protein (CFP or GFP) was ultimately maintained, while in the remaining cases the 100% expresser axon (YFP or CFP) was the surviving input (result is not significantly different from chance, within a 95% confidence interval using a Bernoulli trials process). In addition, controls were performed that indicated that the observed changes were not a result of nerve damage, muscle damage, or phototoxicity associated with the live imaging (see below).

Synaptic Takeover

In all two-color junctions ($n = 24$), the process appeared to be the same; one input withdrew from postsynaptic sites and the other input elaborated new branches that replaced lost synaptic terminals at most of those sites. This competitive process usually took days to reach completion. Takeover and withdrawal seemed closely

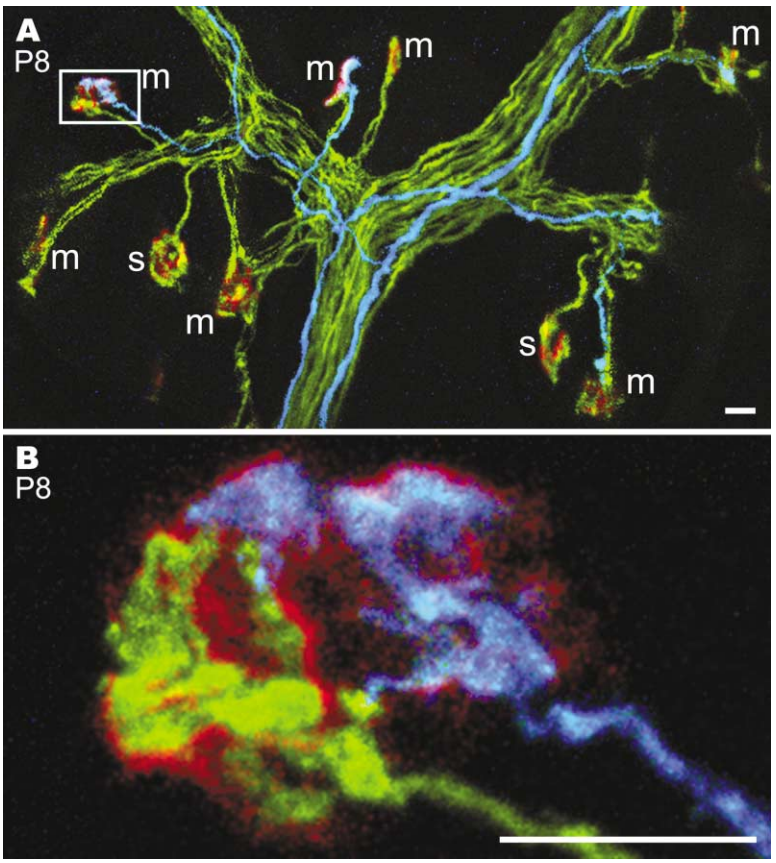

Figure 1. Expression of Different Fluorescent Proteins in Different Motor Axons in Double Transgenic Mice

In this muscle, all motor axons express YFP (yellow), and a small random subset expresses CFP (blue). A red-shifted fluorescent α-btx was added to label the AChRs in the postsynaptic membrane (red).

(A) Low-power image of part of an excised and fixed sternomastoid muscle at P8 in which only one motor axon expressed CFP. Both singly innervated (s) and multiply innervated (m) junctions are visible.

(B) High-power image of the neuromuscular junction shown in box in (A). The CFP containing axonal input is segregated to the right half of the junction. Scale bars equal 10 μm.

coordinated because in none of the junctions were postsynaptic sites temporarily unoccupied. It should be noted, however, that the exact temporal relationship between expansion and withdrawal could not be discerned unambiguously in this work because both axons expressed one of the fluorescent proteins, and hence the degree to which the terminal branches of the competing axons overlapped could not be determined. Two examples of takeover and withdrawal are shown in Figure 2. In each case the postsynaptic acetylcholine receptor (AChR) areas remain largely unchanged as the source of innervation is exchanged. In all of the two-color junctions followed, the sites of synaptic exchange occurred at the boundaries of the territories occupied by the two inputs, i.e., the remaining axon never leapt over its competitor to acquire noncontiguous territory. In each case there appeared to be considerable dynamism of axon branch length and caliber, even in branches that were not in the process of withdrawing or acquiring new territory (Figures 2A–2E, insets).

Surprisingly, in 6/24 two-color junctions, the input that ultimately was maintained appeared to possess $\sim$30% or less ($<$50 μm^2, estimate does not include potential overlap, see above) of the total terminal area at some earlier time point (Figures 2F–2J, 3A, and 3B). In one junction the surviving axon increased its territory dramatically from occupying only $\sim$20 μm^2 ($\sim$10%) at the initial view to $\sim$200 μm^2 (100%) of the terminal area 5 days later (Figures 3A and 3B).

The speed of takeover could be quite rapid. The largest 1 day change we observed was an axon whose junctional branches had $\sim$30% ($\sim$30 μm^2) of the total terminal area on one day and all of the area ($\sim$100 μm^2) 24 hr later (233% increase). The median increase in area per day was $\sim$40 μm^2 ($\sim$25% of terminal area). The amount of takeover per day varied considerably among different junctions and among time points at individual junctions (e.g., Figures 2C and 2D versus 2D and 2E), and in some cases there was virtually no change in terminal areas over 1 day intervals (6/21 1 day intervals monitored).

Flip-Flop

Although in some junctions (see Figures 2, 3A, and 3B) synaptic takeover appeared to progress monotonically until single innervation was achieved, in three junctions we observed flip-flop; an input that lost territory, then regained it (Figures 3C–3F). However, once axons had completely withdrawn from junctions, in no cases did they reform synapses on those junctions.

In addition, sites taken over by an axon during the second postnatal week were stably maintained once takeover was complete. We continued to image five junctions for several additional weeks or months (P30–P146). In all cases, we found that the areas that had been taken over during the second postnatal week were still innervated by that axon in adulthood (data not shown).

Dynamism in Singly Innervated Junctions

These results suggest that when synapse elimination is occurring, axons are highly dynamic. This dynamism

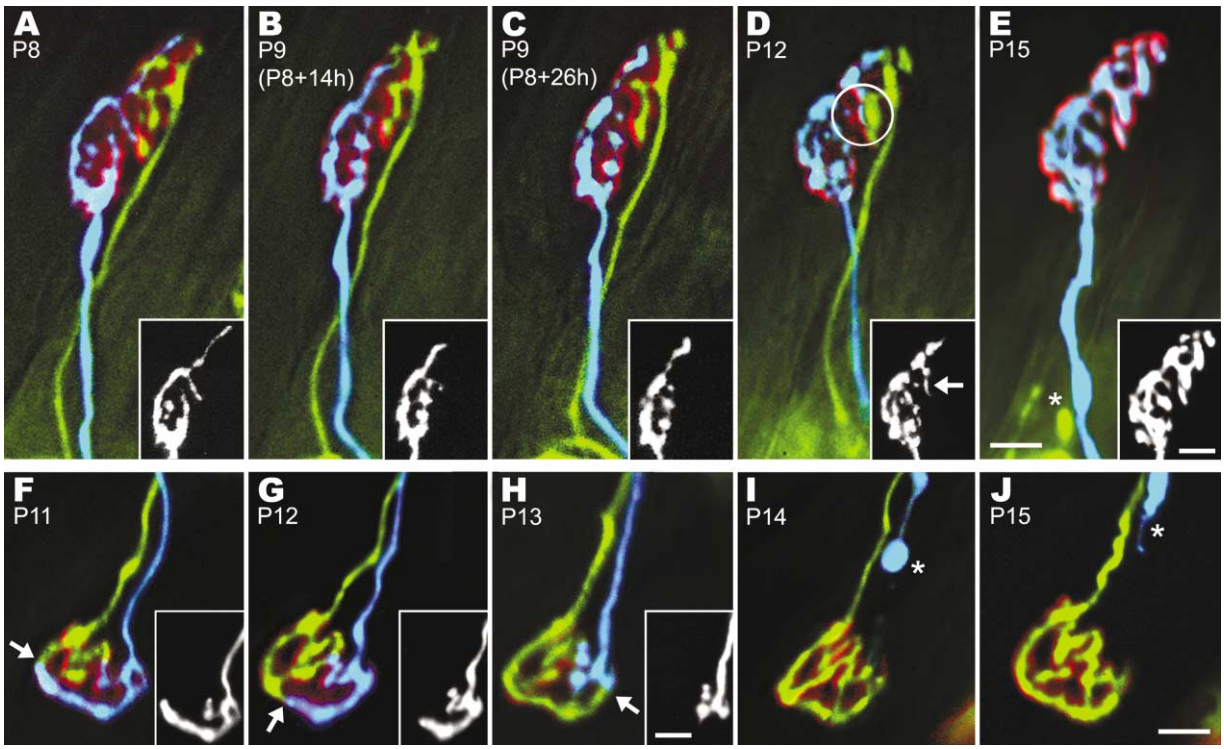

Figure 2. Synaptic Takeover

In vivo imaging of the same multiply innervated junctions in neonates provides evidence both for the gradual relinquishment of synaptic territory by the losing axon before it is eliminated and takeover by the winning axon of synaptic territory that previously was occupied by the losing axon.

(A–E) Five views of the same junction imaged between P8 and P15. The subset CFP axon (blue) comes to occupy the sites in the upper parts of the junction that were formerly innervated by the YFP axon (yellow; 100% expresser), which completely withdrew (E, asterisk). At P12, a process of the CFP axon had begun to invade the territory of the YFP axon (D, circle and arrow in inset).

(F–J) Although in this case the subset CFP axon (blue and insets) has greater terminal area (~70%) at the first view, it progressively withdraws from the junction (arrows). The withdrawn axon can be seen in (I) and (J) (asterisks). Insets, 70% size reduction. Scale bars equal 10 μm.

contrasts with the stability of axon terminals at singly innervated junctions in this same muscle in adult mice (Balice-Gordon and Lichtman, 1990; Robbins and Polak, 1988). To determine whether synaptic competition between axons is causing the dynamic behavior of axons, we monitored neuromuscular junctions that were already singly innervated in the second postnatal week in order to see whether these terminals also exhibited dynamic behavior. Singly innervated junctions in the second postnatal week ($n = 30$) were all highly dynamic (Figures 4A–4C), exhibiting process extensions, retractions, and terminal caliber changes over intervals of 24 hr. On the other hand, 2 weeks later (P21–P28), singly innervated junctions ($n = 13$) were quite stable and over the 3–4 day imaging sessions, none showed new branch formation, branch retraction, or caliber changes, suggesting that the dynamic behavior had dramatically decreased (Figures 4D–4F). This reduction contrasts with the maintained plasticity of adult amphibian neuromuscular junctions (Herrera et al., 1990; Wernig et al., 1980).

Synapse Elimination without Takeover

We observed several junctions (4/28) in which vacated synaptic sites were not taken over by the remaining axon (Figures 5A–5C). In Figure 5A is a multiply innervated neuromuscular junction at P10 in which two inputs (labeled the same color) occupy segregated and noncontiguous postsynaptic AChR sites of the same muscle fiber. At the second view (P14), the input that had the lesser amount of territory at P10 had retracted (asterisk) and its vacated site lost substantial AChR density (compare arrows, Figures 5A and 5B). By P21 the AChRs at the vacated site had been completely removed. Another junction with noncontiguous postsynaptic territories (not shown) had essentially the identical outcome. In 2 two-color junctions, the transition from multiple to single innervation was accompanied by the takeover of only a portion of the vacated postsynaptic territory. In all four cases, the vacated synaptic sites that were not reoccupied lost all signs of AChR labeling rapidly and completely. These results show that synaptic takeover is not required for synapse elimination to occur and further suggest that rapid destabilization of synaptic sites occurs when they are not taken over by the remaining axon.

In order to better understand what caused the disappearance of AChRs at unoccupied sites, we compared AChR disappearance at sites that were not reoccupied during synapse elimination with AChR disappearance after complete denervation. When a muscle was imaged and denervated at P10 and then imaged again 4 days later (P14), there was little change in AChR density

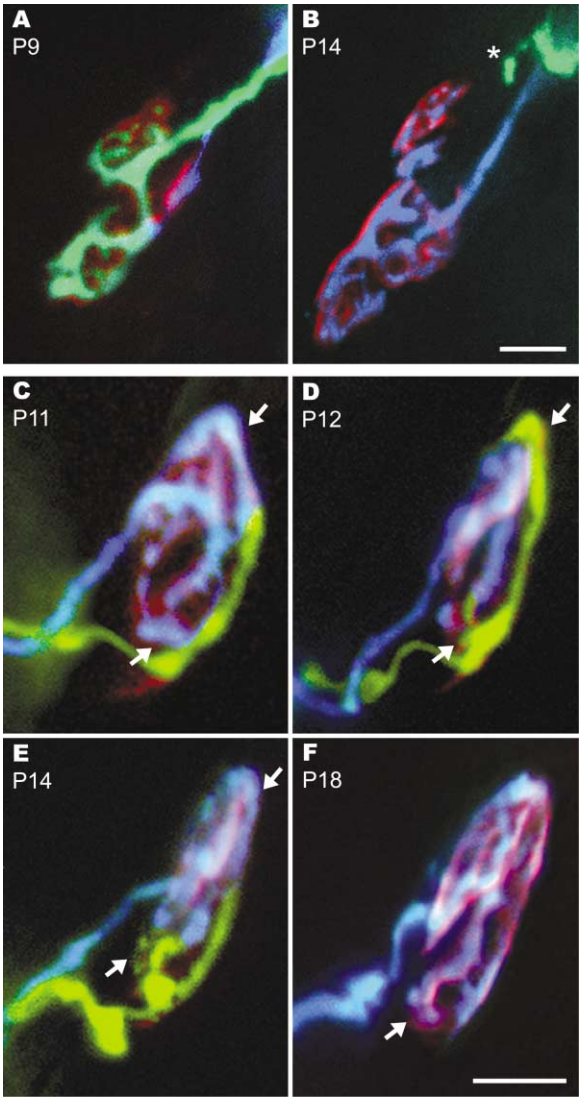

Figure 3. Dramatic Reversals and Flip-Flop in Nerve Terminal Area during Synapse Elimination

(A and B) Junction in which the GFP input (green; subset) occupies nearly all of the junction at P9 (~90%) but nonetheless was completely eliminated by P14 (note retraction bulb asterisk in B).

(C–F) Junction exhibiting flip-flop. The subset CFP axon (blue) loses and then regains postsynaptic territory. Between P11 (C) and P12 (D), the CFP axon relinquished some of its territory to the YFP (yellow; 100% expresser) input (compare arrows in C and D). By P14 (E), it has reclaimed the upper right portion of the junction but continued to retreat from the lower part of the junction (compare arrows in D and E). At P18 (F), the CFP input had reclaimed all of its former territory and had taken over the postsynaptic territory previously occupied by the YFP input. The thinner appearance of the junction after P11 is due to slight muscle fiber rotation. Scale bars equal 10 μm.

(~10% decrease) at these neuromuscular junctions. This result is dramatically different from the fate of unoccupied AChRs at sites of synapse elimination (e.g., Figures 5A–5C) that substantially decreased (~90% decrease) in density between P10 and P14. Because rapid receptor site disassembly is not caused by denervation per se, these results support the idea that some kind of intersynaptic signaling permits one axon's synaptic sites to destabilize synaptic sites of competing axons. Thus, rapid synaptic takeover appears to rescue postsynaptic sites that would otherwise rapidly disassemble.

Discussion

Throughout the developing nervous system, axons disconnect from target cells in a phenomenon known as synapse elimination. This study indicates that the loss of synaptic contacts by axons that withdraw during naturally occurring synapse elimination is actually just one component of a larger coordinated process that also includes expansion of synaptic area by competing axons. The expansion of synaptic territory, however, occurred exclusively at former postsynaptic sites relinquished by another axon. Such replacement obviates the need for generating new postsynaptic sites as axons expand their territory, and thus provides a means for rapid synaptic enhancement.

Because larger synapses are often associated with greater neurotransmitter release (Costanzo et al., 1999; Kuno et al., 1971), it is possible that the expansion of synaptic territory associated with takeover increases the synaptic strength of the remaining input. This expansion is therefore likely to be the basis for previously reported increases in quantal content during synapse elimination in muscle (Colman et al., 1997). Additionally, takeover may provide a structural explanation for the large increases in synaptic strength that occur concurrently with developmental synapse elimination in thalamus (Chen and Regehr, 2000), autonomic ganglia (Lichtman, 1977), the cerebellum (Mariani and Changeux, 1981), and the avian auditory system (Jackson and Parks, 1982).

This work also suggests that synaptic terminal removal is possible without obvious effects on the underlying postsynaptic apparatus, which at sites of takeover seems to be stable. This result was unexpected. In our previous attempts to follow synapse elimination over time, all axons were fluorescently labeled the same color, and due to the close proximity of competing axons, synaptic takeover was not detected (Balice-Gordon and Lichtman, 1993; Rich and Lichtman, 1989). Rather, in previous studies the only clear signs of synapse elimination were at sites in which both axon terminal and postsynaptic AChR loss were observed. The present work, however, suggests that AChR loss may only occur when synaptic takeover fails (e.g., Figure 5). Nonetheless, the AChR loss seen here and previously does provide several insights into the underlying signaling cascade causing axons to withdraw. First, the observation that axons can withdraw from sites that are not taken over by the other input rules out the idea that synapse elimination requires one axon to displace another from a synaptic site. Second, because the rapid disappearance of AChRs at former synaptic sites could not be explained simply by the absence of overlying nerve terminals (see Figure 5), we suspect that unoccupied postsynaptic sites are efficiently dismantled in response to synaptic activity at occupied synaptic sites on the same postsynaptic cell as previously suggested (Balice-Gordon and Lichtman, 1994). Presumably synaptic takeover

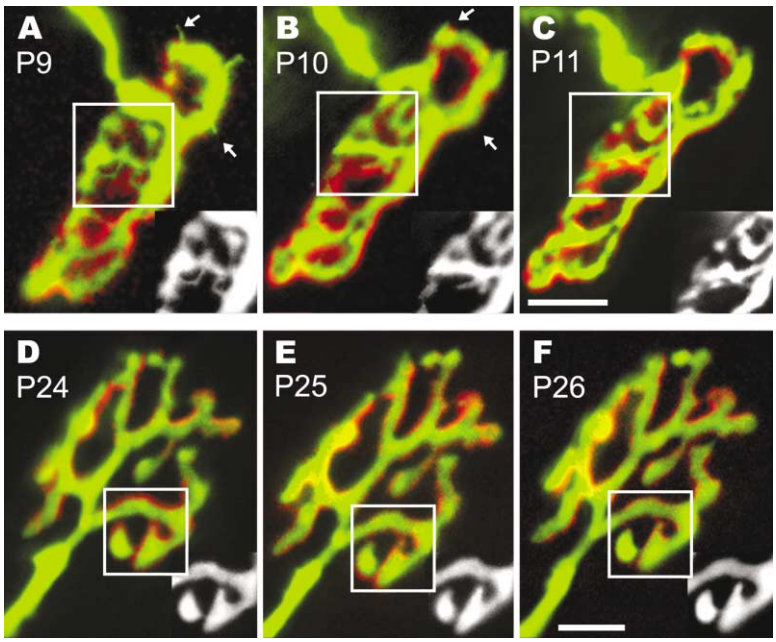

Figure 4. Dynamic Changes in Axon Terminals at Singly Innervated Neonatal Junctions

(A–C) A singly innervated junction imaged from P9–P11. Changes over time in the branching and caliber of terminals are evident (see inset boxes also). Sprouts extending beyond the confines of the AChR plaque present at P9 retracted by P10 (compare arrows in A and B).

(D–F) Axon terminals in this slightly older junction (P24–26) show fewer alterations in caliber or branching (see inset boxes also). Scale bars equal 10 μm.

conserves postsynaptic sites by rapid reoccupation before the AChR density is removed.

It is not clear what stimulates an axon to takeover neighboring postsynaptic sites. One possibility is that the process of axonal withdrawal may induce another axon to grow toward those sites, perhaps in response to secreted growth factors that become available. Alternatively, axons may rapidly replace competitors if they have a high degree of intrinsic dynamism. For example, young axons may continually explore the postsynaptic territory and thus are usually available to occupy sites when they become vacant. These results support this latter alternative because all young axons, even those in singly innervated completely occupied junctions, were dynamic and many possessed sprouts that extended away from postsynaptic sites (e.g., see arrows, Figure 4A).

Unexpectedly, the relative amount of territory occupied by each axon was not a reliable predictor of which axon would ultimately be maintained, as axons occupying large fractions of the total junctional territory sometimes were replaced by axons occupying smaller areas. Moreover, the takeover process itself often did not progress monotonically, as an axon that was advancing was sometimes observed to then retreat. One interpretation of these behaviors is that an axon's com-

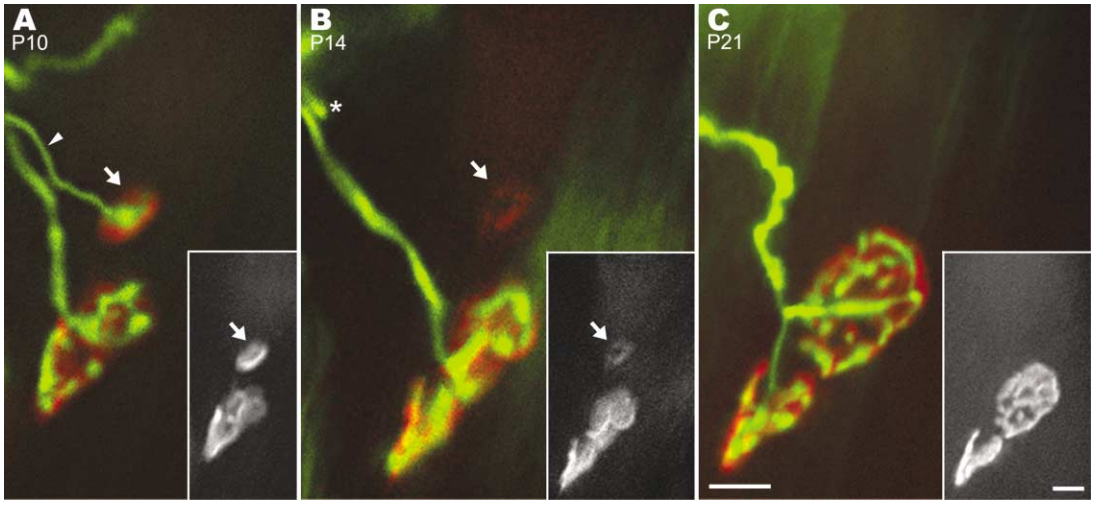

Figure 5. Synapse Elimination without Takeover

This muscle fiber is multiply innervated at P10 (A) by two YFP axons, one of which is atrophic (arrowhead) and occupies a relatively small postsynaptic territory. By P14 (B) this axon retracted (asterisk), but its postsynaptic site was not taken over by the remaining input. Instead, the AChRs at that site have started to disappear (A and B, compare arrows), and by P21 there were no AChRs present in that area (C). AChRs were relabeled at P14 (B) and P21 (C). Insets, AChR-labeling only, 50% reduction. Scale bars equal 10 μm.

petitive vigor can change dramatically over the several day time course of this synaptic competition. One possible explanation for the flip-flop is that the growth potential of a terminal branch at one junction may change as resources become available or lost due to the outcome of competitions occurring simultaneously in other branches of the neuron (Barber and Lichtman, 1999).

It has long been known that in experimental situations one axon can reinnervate postsynaptic sites that were previously occupied by another axon in both the CNS (Chen and Hillman, 1982) and PNS (Saito and Zacks, 1969). Several studies suggest that following nerve damage in adult animals, regenerating motor axons can competitively replace existing nerve terminals at neuromuscular junctions (Bixby and Van Essen, 1979; Costanzo et al., 2000). The present results provide evidence that such presynaptic replacement is an integral part of the normal maturation of neuromuscular junctions.

In conclusion, synaptic takeover is a mechanism by which an input can quickly increase its synaptic area and hence synaptic strength by taking advantage of previously occupied postsynaptic sites. Input withdrawal and synaptic takeover appear to be two sides of the same coin: a single developmental strategy by which an axonal input can weaken its neighbor while at the same time increasing its own synaptic strength.

Experimental Procedures

Animals

Transgenic mice expressing spectral variants of cytoplasmic GFP in motor neurons were used (Feng et al., 2000). Mice that expressed either cytoplasmic CFP (lines CFP-D$^{+/-}$ or CFP-5$^{+/-}$) or YFP (YFP-F$^{+/+}$ or YFP-16$^{+/+}$) in all motor neurons (100% expressers) were crossbred with mice that expressed cytoplasmic GFP (initially line GFP-S$^{+/-}$ and then subsequently GFP-S$^{+/+}$) or CFP (CFP-S$^{+/-}$ then CFP-S$^{+/+}$), respectively, in subsets of motor axons (subset expressers). The resultant double transgenic mouse pups were used for all experiments (protocol approved by Washington University Animal Studies Committee).

Fixed Tissue Imaging

We deeply anesthetized double transgenic neonatal mice with an intraperitoneal (i.p.) injection of sodium pentobarbital (Nembutal, Abbott Laboratories, North Chicago, IL; ~1 mg/gm of body weight) and then transcardially perfused them with 2%–4% paraformaldehyde in 0.1 M phosphate-buffered saline (PBS; pH 7.4). We then removed the sternomastoid muscles and incubated them in 5 μg/ml of Alexa Fluor 594 conjugated α-bungarotoxin (α-btx; Molecular Probes, Eugene, OR) in PBS with 1% bovine serum albumin for 10 min to saturate AChRs. Muscles were rinsed in PBS at room temperature for 1 hr and mounted on slides in Vectashield mounting medium (Vector Laboratories, Burlingame, CA). We then imaged the muscles using a confocal laser scanning microscope (BioRad 1024, Hercules, CA; Olympus BX50WI microscope). Figures 1A and 1B were obtained using a 40× 1.35 NA oil objective and a 100× 1.4 NA oil objective, respectively. Maximum pixel projections were generated from Z stacks of images using Metamorph 4.6 imaging software (Universal Imaging Corp., West Chester, PA).

In Vivo Time-Lapse Imaging

We anesthetized neonatal mice, usually starting at the beginning of the second postnatal week (P8 [n = 7], P9 [n = 12], or P11 [n = 5]) by subcutaneous injection of a mixture of ketamine (K; Ketaset, Fort Dodge Animal Health, Fort Dodge, IA) and medetomidine (M; Domitor, Orion Corp., Espoo, Finland; KM cocktail, 1.7 mg K + 0.23 mg M/ml of sterile saline; dosage, ~0.1 ml for 5 gm animal, ~0.25 ml for 10 gm animal). Mice were then intubated with a small polyethylene tube, mechanically respirated (80/min; MiniVent Type 845, Hugo Sachs Electronik, Germany), and warmed on a temperature-controlled heating element. Mouse pups were handled with latex gloves to avoid rejection/cannibalization when returned to parents at the end of each imaging session. We removed any hair on the ventral neck with depilatory cream. Using aseptic technique, the right and left sternomastoid muscles were exposed in the ventral neck (Lichtman et al., 1987). Approximately 3% (determined by quantitative fluorescence) (Turney et al., 1996) of the postsynaptic AChRs were then labeled with fluorescently conjugated α-btx (2 min of 0.5 μg/ml Alexa Fluor 594 α-btx, followed by rinsing with 30 ml physiological lactated Ringer's, Baxter Healthcare Corp., Deerfield, IL). Given the large safety factor of the neuromuscular junction even in neonates (>40% of AChRs must be blocked to disrupt transmission) (Wareham et al., 1994), this dosage should not block postsynaptic activity. We slightly elevated the sternomastoid muscle on a flat polished steel platform attached to a small manipulator. A rubber O-ring was gently placed on the ventral surface of the muscle surrounding the central band of neuromuscular junctions to both stabilize the muscle and provide a water well for the immersion objectives. Low-magnification maps (10×, 0.3 NA water objective) of the band of junctions and higher-power (60×, 1.0 NA water objective) images of individual junctions were taken using a standard epifluorescence microscope (Nikon Eclipse E800) with a cooled CCD camera (Roper Scientific Princeton Instruments MicroMAX:512BFT thinned, back-illuminated, Trenton, NJ). Exciting wavelengths were provided by a xenon lamp and rapidly switched exciting filters (Lambda DG-4, Sutter Instrument Co., Novato, CA; filters, Chroma Technology Corp., Brattleboro, VT). Stacks of images (1 μm steps) of individual junctions were obtained (piezoelectric objective Z-axis stepper, Physik Instrumente, Waldbronn, Germany). For three-color junctions (two differently labeled axons and fluorescent bungarotoxin-labeled postsynaptic sites), a triple dichroic (Chroma XF91) was used to rapidly obtain all three colors at each image plane without having to switch filters. The respirator was turned off briefly (<30 s) during stack acquisition to minimize movement. Each image was acquired in 0.1–0.5 s. Separate stacks were also obtained for each of the three colors using single dichroics (Chroma) chosen to maximize separation among the various fluorophores: YFP and GFP (exciter-HQ500/20x, dichroic-Q515LP, emitter-HQ535/30m), CFP (exciter-D436/20x, dichroic-455DCLP, emitter-D480/40m), and red-shifted Alexa Fluor 594 α-btx (exciter-D560/40x, dichroic-595DCLP, emitter-D630/60m). These dichroics easily separated fluorescent proteins from labeled AChRs and also separated CFP from YFP and most notably GFP from CFP. The single dichroic images were used to generate composite images, using the triple dichroic images as an alignment reference. Two-dimensional images were derived from stacks of images by extracting in-focus information from each image plane to create image mosaics. Terminal area percentages were determined by tracing presynaptic profiles apposed to AChRs and then calculating areas. After completing an imaging session (typically 1 hr), we sutured the wound (9-0 Ethilon monofilament nylon, Ethicon Inc., Somerville, NJ), and gave the animal an i.p. injection of atipamezole (Antisedan, 0.25 mg/ml of sterile saline, ~0.05 ml/5 gm of body weight, Orion Corp.) to reverse the effects of medetomidine and to decrease the chances of anesthetic overdose and a subcutaneous injection of 0.1 ml sterile lactated Ringer's to prevent dehydration. The animal was placed on a heated blanket in a 95% oxygenated chamber until sufficiently recovered and active (usually less than 2 hr), at which time it was returned to its parents. The animal was allowed to recover for a variable amount of time (several hours to several days; median interval, 2 days; median number of views per junction, 3.5) before reimaging. At subsequent sessions, we reanesthetized mice and the previously imaged junctions were easily relocated using the low-power maps. The entire image acquisition procedure was repeated at each session. Due to natural AChR turnover, relabeling of AChRs was often necessary after several days (e.g., Figures 2E, 2I, 3B, 3F, 5B, and 5C).

In control experiments, we found that damage to the nerve (nerve crush lateral to muscle) resulted in discontinuous or beaded fluorescence in axons within 24 hr with most junctions no longer apposed by any fluorescence. Damage to the muscle (crush at middle of muscle, which may include direct nerve damage also) sometimes resulted in long terminal and/or nodal sprouts (some greater than 100 μm within 2 days). Less than 5% of animals repeatedly imaged

showed either of these signs of damage, and in all of these cases the damage was obvious at the time it was inflicted. All damaged preparations were excluded from analysis. We also tested for phototoxicity. In neonatal muscles, CFP, GFP, YFP, and fluorescent α-btx were illuminated in vivo continuously at full intensity for 1 hr at the appropriate excitation wavelengths (60× 1.0 NA water immersion objective). Although this dose of excitation was one to two orders of magnitude greater than junctions normally receive during imaging, no signs of damage or phototoxicity (not even photobleaching) were seen either immediately or after 24 hr. These controls indicate that the dynamic changes observed in these studies are not induced by nerve-, muscle-, or photo-damage. Moreover, the junctions that were imaged multiple times (up to 10 times) showed no pre- or postsynaptic structural features that were not seen in age-matched junctions imaged only once.

Acknowledgments

We would like to thank the members of our lab for many helpful discussions and J. Tollett and S.G. Turney for technical assistance. We thank J.R. Sanes and G. Feng for generating the transgenic mice. This work was supported by grants from the NIH and Muscular Dystrophy Association to J.W.L. and by generous support from the Bakewell NeuroImaging Fund.

Received: September 27, 2002
Revised: November 15, 2002

References

Balice-Gordon, R.J., and Lichtman, J.W. (1990). In vivo visualization of the growth of pre- and postsynaptic elements of neuromuscular junctions in the mouse. J. Neurosci. *10*, 894–908.

Balice-Gordon, R.J., and Lichtman, J.W. (1993). In vivo observations of pre- and postsynaptic changes during the transition from multiple to single innervation at developing neuromuscular junctions. J. Neurosci. *13*, 834–855.

Balice-Gordon, R.J., and Lichtman, J.W. (1994). Long-term synapse loss induced by focal blockade of postsynaptic receptors. Nature *372*, 519–524.

Barber, M.J., and Lichtman, J.W. (1999). Activity-driven synapse elimination leads paradoxically to domination by inactive neurons. J. Neurosci. *19*, 9975–9985.

Bixby, J.L., and Van Essen, D.C. (1979). Competition between foreign and original nerves in adult mammalian skeletal muscle. Nature *282*, 726–728.

Chen, S., and Hillman, D.E. (1982). Plasticity of the parallel fiber-Purkinje cell synapse by spine takeover and new synapse formation in the adult rat. Brain Res. *240*, 205–220.

Chen, C., and Regehr, W.G. (2000). Developmental remodeling of the retinogeniculate synapse. Neuron *28*, 955–966.

Colman, H., Nabekura, J., and Lichtman, J.W. (1997). Alterations in synaptic strength preceding axon withdrawal. Science *275*, 356–361.

Costanzo, E.M., Barry, J.A., and Ribchester, R.R. (1999). Co-regulation of synaptic efficacy at stable polyneuronally innervated neuromuscular junctions in reinnervated rat muscle. J. Physiol. *521*, 365–374.

Costanzo, E.M., Barry, J.A., and Ribchester, R.R. (2000). Competition at silent synapses in reinnervated skeletal muscle. Nat. Neurosci. *3*, 694–700.

Feng, G., Mellor, R.H., Bernstein, M., Keller-Peck, C., Nguyen, Q.T., Wallace, M., Nerbonne, J.M., Lichtman, J.W., and Sanes, J.R. (2000). Imaging neuronal subsets in transgenic mice expressing multiple spectral variants of GFP. Neuron *28*, 41–51.

Gan, W.B., and Lichtman, J.W. (1998). Synaptic segregation at the developing neuromuscular junction. Science *282*, 1508–1511.

Herrera, A.A., Banner, L.R., and Nagaya, N. (1990). Repeated, in vivo observation of frog neuromuscular junctions: remodelling involves concurrent growth and retraction. J. Neurocytol. *19*, 85–99.

Jackson, H., and Parks, T.N. (1982). Functional synapse elimination in the developing avian cochlear nucleus with simultaneous reduction in cochlear nerve axon branching. J. Neurosci. *2*, 1736–1743.

Katz, L.C., and Shatz, C.J. (1996). Synaptic activity and the construction of cortical circuits. Science *274*, 1133–1138.

Kuno, M., Turkanis, S.A., and Weakly, J.N. (1971). Correlation between nerve terminal size and transmitter release at the neuromuscular junction of the frog. J. Physiol. *213*, 545–556.

Lichtman, J.W. (1977). The reorganization of synaptic connexions in the rat submandibular ganglion during post-natal development. J. Physiol. *273*, 155–177.

Lichtman, J.W., Magrassi, L., and Purves, D. (1987). Visualization of neuromuscular junctions over periods of several months in living mice. J. Neurosci. *7*, 1215–1222.

Lohof, A.M., Delhaye-Bouchaud, N., and Mariani, J. (1996). Synapse elimination in the central nervous system: functional significance and cellular mechanisms. Rev. Neurosci. *7*, 85–101.

Mariani, J., and Changeux, J.P. (1981). Ontogenesis of olivocerebellar relationships. I. Studies by intracellular recordings of the multiple innervation of Purkinje cells by climbing fibers in the developing rat cerebellum. J. Neurosci. *1*, 696–702.

Purves, D., and Lichtman, J.W. (1980). Elimination of synapses in the developing nervous system. Science *210*, 153–157.

Rich, M.M., and Lichtman, J.W. (1989). In vivo visualization of pre- and postsynaptic changes during synapse elimination in reinnervated mouse muscle. J. Neurosci. *9*, 1781–1805.

Robbins, N., and Polak, J. (1988). Filopodia, lamellipodia and retractions at mouse neuromuscular junctions. J. Neurocytol. *17*, 545–561.

Saito, A., and Zacks, S.I. (1969). Fine structure of neuromuscular junctions after nerve section and implantation of nerve in denervated muscle. Exp. Mol. Pathol. *10*, 256–273.

Turney, S.G., Culican, S.M., and Lichtman, J.W. (1996). A quantitative fluorescence-imaging technique for studying acetylcholine receptor turnover at neuromuscular junctions in living animals. J. Neurosci. Methods *64*, 199–208.

Wareham, A.C., Morton, R.H., and Meakin, G.H. (1994). Low quantal content of the endplate potential reduces safety factor for neuromuscular transmission in the diaphragm of the newborn rat. Br. J. Anaesth. *72*, 205–209.

Wernig, A., Pecot-Dechavassine, M., and Stover, H. (1980). Sprouting and regression of the nerve at the frog neuromuscular junction in normal conditions and after prolonged paralysis with curare. J. Neurocytol. *9*, 278–303.